Result and Validation

4.1 Introduction

Chapter 2 has dealt with the analytical method for the SSFP-PMSG and MCDSFP-PMSG for the design optimization and determination of electromagnetic performance. The analytical method is fast and reasonably reliable as confirmed by FEM results. Using the analytical method proper selection of stator and rotor core materials, windings, winding insulation, grade of PM are possible. Keeping the pros and cons in mind, two PMSGs namely SSFP-PMSG and MCDSFP-PMSG are fabricated as reported in Chapter 3. The electromagnetic performances calculated from the analytical and FEM needs to be validated for proper understanding of the developed generator.

The main objective of this Chapter is to validate no-load and on-load electromagnetic performance results under healthy and faulty (open circuit of phase) conditions. Section 4.2 deals with the validation of electromagnetic performance with respect to field distribution, generated voltage, and electromagnetic torque under no-load and load condition for SSFP-PMSG. The validation of electromagnetic performances under no-load and loading condition of MCDSFP-PMSG is discussed in Section 4.3. Finally, Section 4.4 concludes this chapter.

4.2 Electromagnetic Performance of SSFP-PMSG

The electromagnetic performances are computed using Reluctance Network Model (RNM), FEM and experimental set-up for SSFP-PMSG. The no-load and load performances like magnetic flux density, generated phase voltage, line voltage, cogging torque, rectified DC voltage have been computed under healthy and faulty (open circuit) conditions.

4.2.1 Magnetic Flux Density of SSFP-PMSG

The Flux density is the building block of designing for a machine and carried out using magnetic circuit approach. This is validated with the FEM magneto-static analysis and further revalidated with the measured results using digital gauss meter (model no.: DGM-102). These results are listed in Table 4.1. The computed airgap flux density using IMC Model is 0.562 Tesla which is 1.316% and 3.41% lesser than FEM and experimental result respectively.

4.2.2 Generated Voltage of SSFP-PMSG

The generated phase voltage using IMC is found 187.56 volts. Fig. 4.1 shows the generated per phase voltage of SSFP-PMSG using analytical, FEM and Experimental results. The generated voltage analytical and simulated FEM results are respectively, 3.28% and 2.02% lesser than the experimental result. Table 4.1 presents these values at rated 400 RPM.

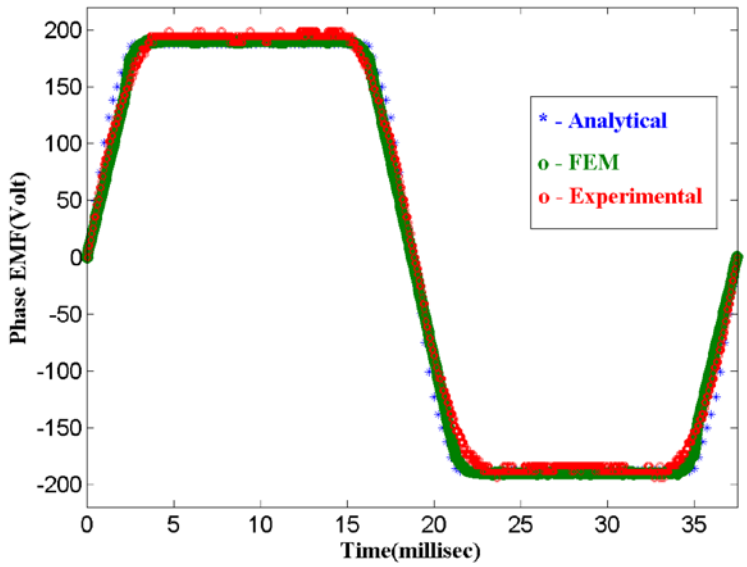

Fig. 4.1 Phase voltage comparison for Analytical, FEM and Experimental results

4.2.3 Cogging Torque of SSFP-PMSG

The cogging torque computed analytically is 4.615 N.m and simulated FEM results are respectively 6.46% and 4% lesser than the experimental results as shown in Fig. 4.2. The computation for the cogging torque in steps of 0.15^{o} in the anticlockwise direction of rotor rotation. For 3 mm of the slot opening the cogging torque, results are given in Table 4.1.

Table 4.1 Analytical, FEM and experimental results of Cogging Torque

Parameter	**Analytical**	**FEM**	**Experimental**	**Unit**
Air gap flux density	0.562	0.5694	0.5812	Tesla
Generated voltage	187.56	190	193.92	Volts
Cogging Torque	4.615	4.736	4.934	N.m

4.2.4 Generated Line Voltage of SSFP-PMSG

The line voltages of the 5-phase PMSG are not same in magnitude and shape. The no-load induced voltage and the line voltage derived analytically at 400 RPM are shown in Fig. 4.3. There are two line voltages V_{ae}; between adjacent phases having 72^{o}E phase separation, and V_{ac}; between non-adjacent phases having 144^{o}E phase separation. The fundamental magnitude of the phase voltage is 187.2 V, and the line voltages between adjacent and non-adjacent phases are 220.2 V and 355.5 V, respectively. Therefore, the fundamental magnitude of line voltage between adjacent phases is 1.176 times the phase voltage, and between non-adjacent phases is 1.90 times the phase voltage. These analytical voltages are in good agreement with the experimental results as shown in Fig. 4.4.

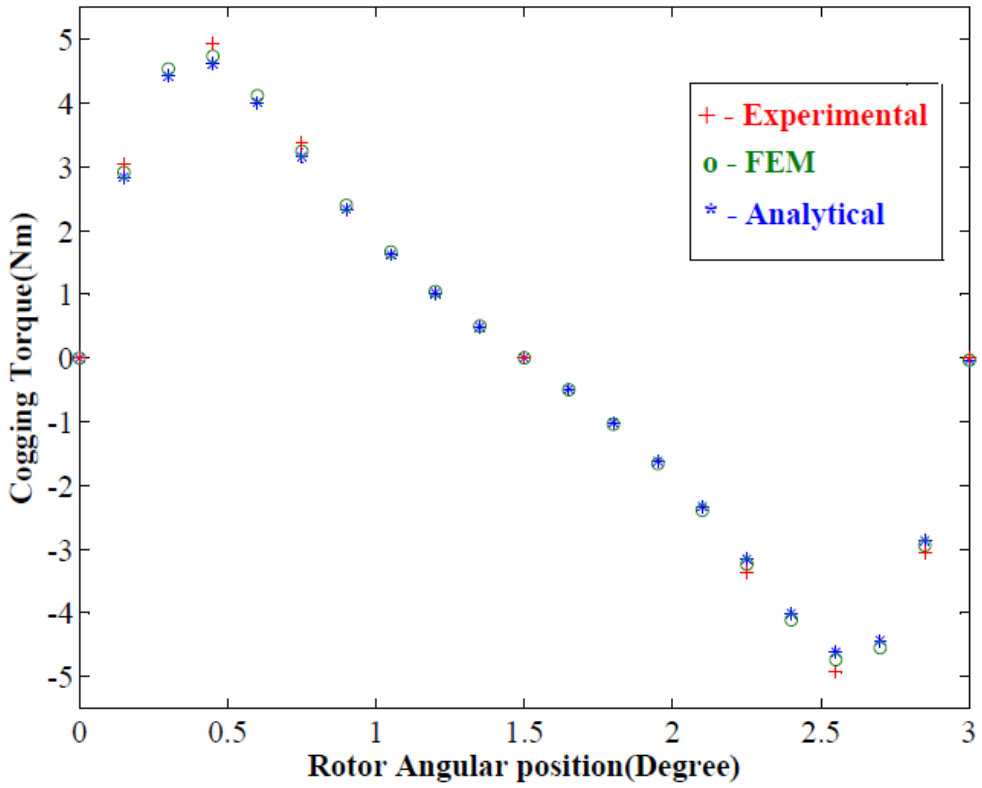

Fig. 4.2 Cogging torque comparison for Analytical, FEM and Experimental results

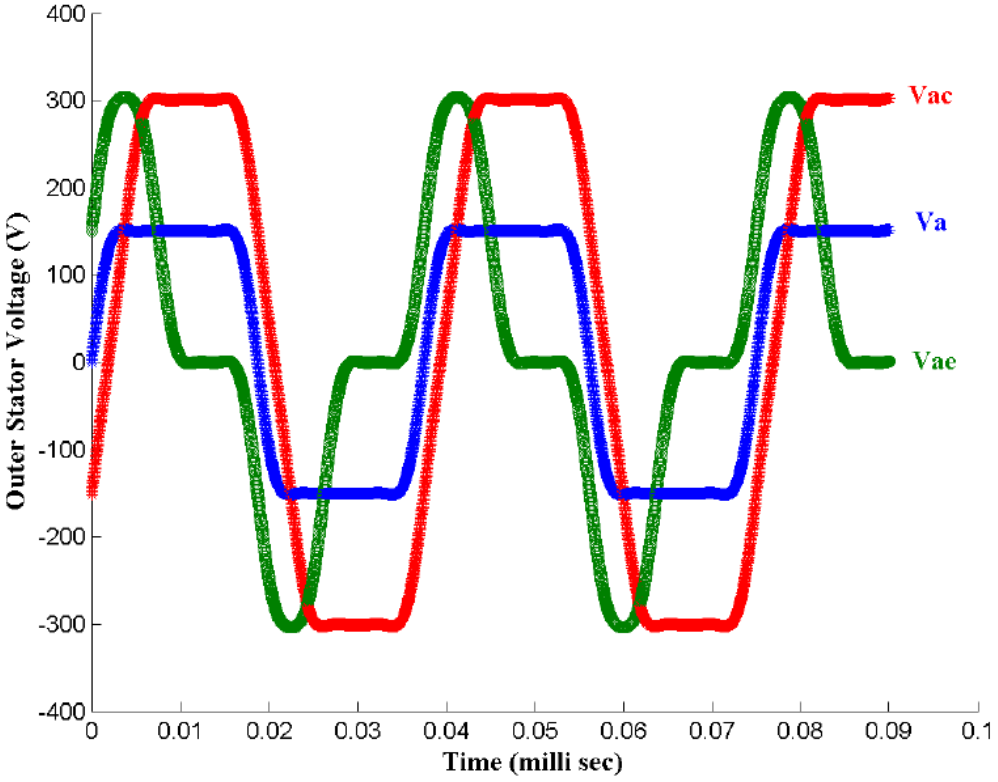

Fig. 4.3 Analytical Phase and line voltages of SSFP-PMSG

4.2.5 Rectified DC Voltage of SSFP-PMSG

Figure 4.5 shows the variation of rectified DC voltage with respect to speed at no-load condition for proposed SSFP-PMSG. A linear relationship is observed between rectified voltage and speed. The rectified DC voltage is found as 386 volts at the rated 400 RPM. The simulated DC Voltage is found in good accordance with the experimental result.

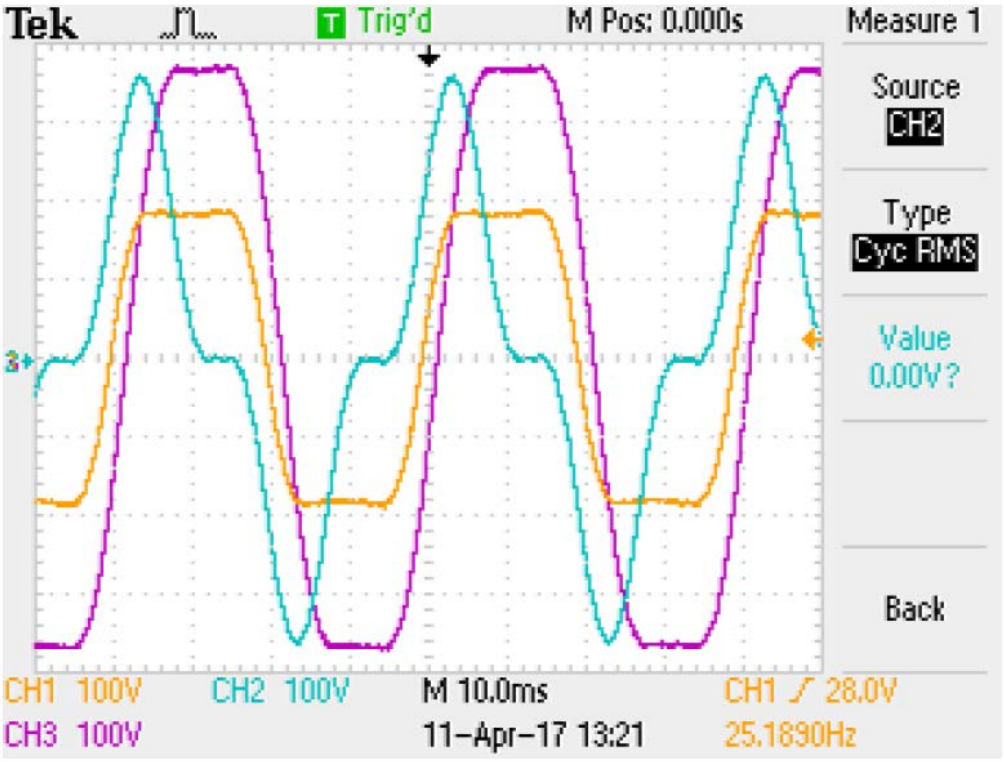

Fig. 4.4 Experimental Phase and line voltages of SSFP-PMSG

The proposed SSFP-PMSG is further loaded using a five-phase diode rectifier upto 4 amps of DC. The drooping DC voltage is due to drop in terminal phase voltage. This is because of armature reaction and internal parameters of the generator. The analytical result is verified with experimental results and found to be of similar profile, but 6.58% lesser than no-load voltage, as shown in Fig.4.6. Further, variation in the

rectified power with a resistive load is shown in Fig. 4.7. It is found that the analytical result is in good agreement with the experimental result.

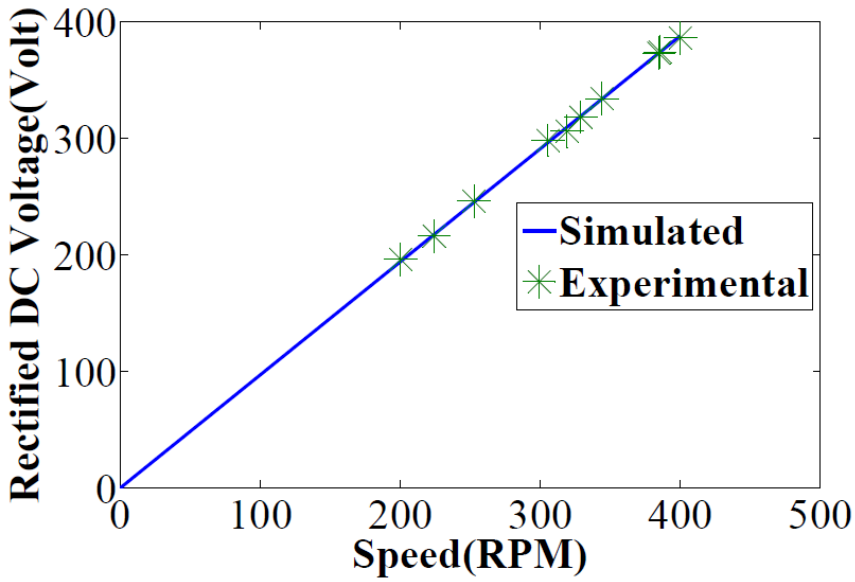

Fig. 4.5 Rectified DC Voltage vs. Speed

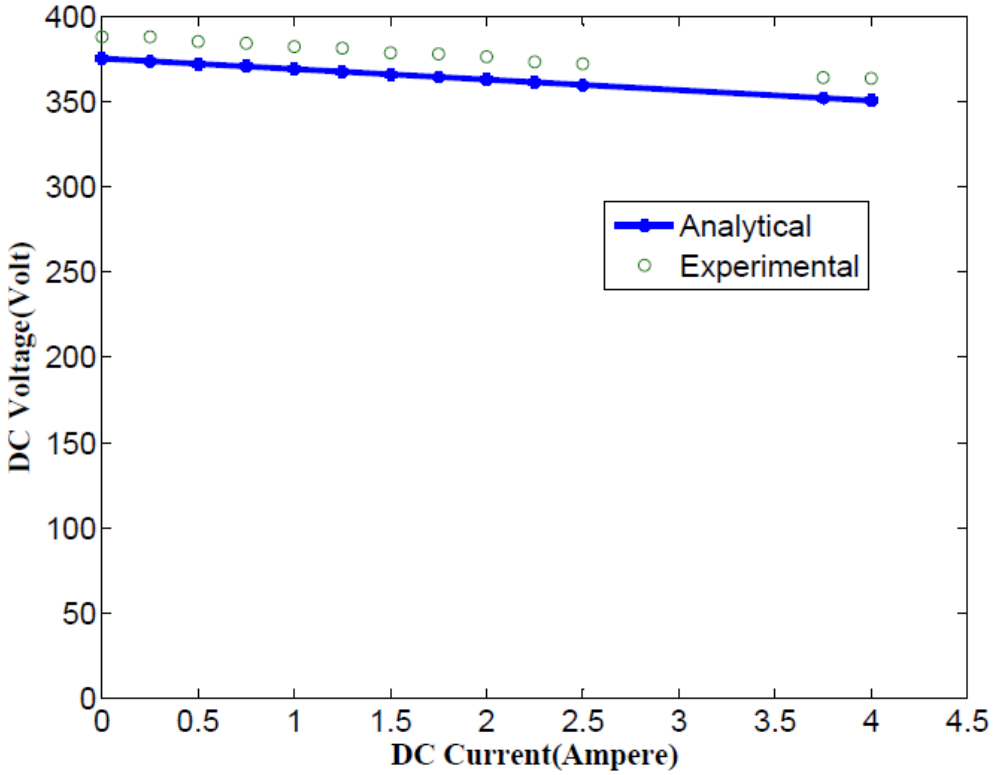

Fig. 4.6 DC Voltage vs. DC Current

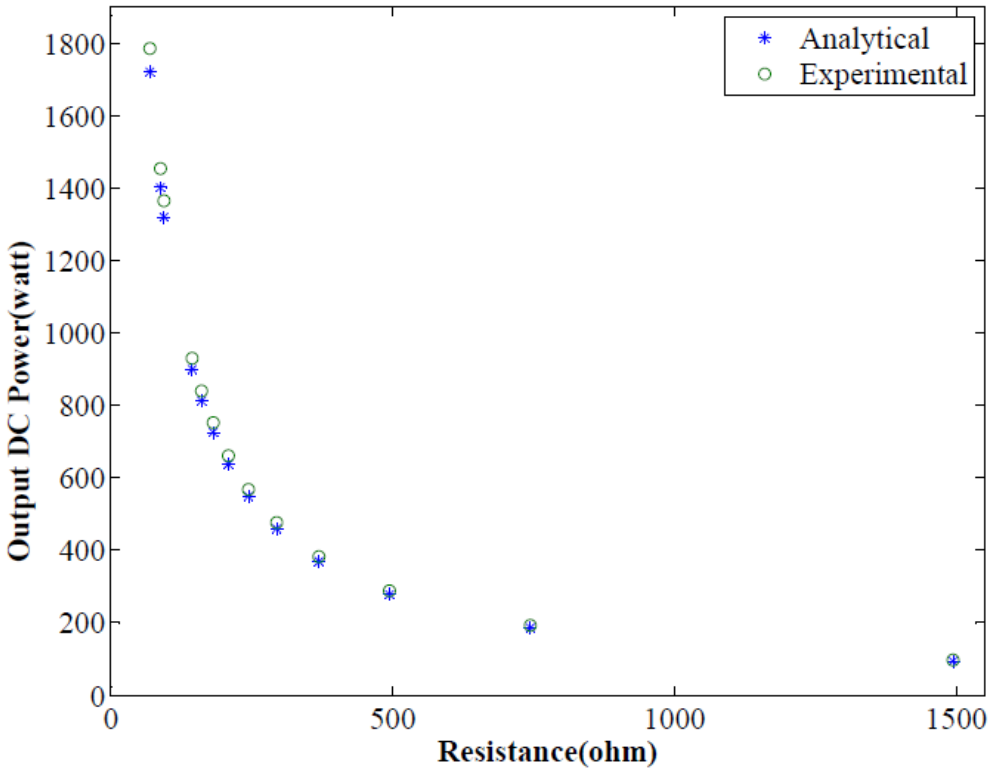

Fig. 4.7 Output DC power vs Load resistance

4.2.6 Electromagnetic torque of SSFP-PMSG

Figure 4.8 shows the simulated and FEM results of electromagnetic torque. The simulated torque is found 2.46% higher than the FEM torque of 81.86 N.m obtained from FEM at 400 RPM. The torque ripple is 8.62 % and 7.4% for simulated and FEM results, respectively.

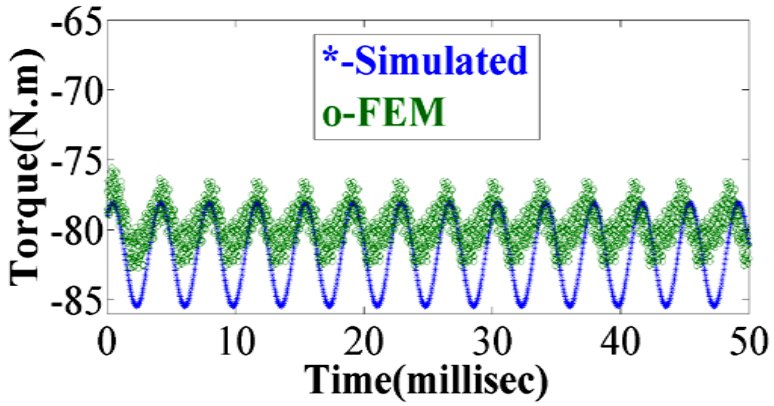

Fig. 4.8 Electromagnetic torque of SSFP-PMSG

4.3 Electromagnetic performance of MCDSFP-PMSG

The electromagnetic performances of MCDSFP-PMSG have been calculated using ananalytical method and have been validated with FEM results. For knowing the level of accuracy the experiment has to be conducted with the prototype generators.

4.3.1 Generated voltage of MCDSFP-PMSG

The generated voltages in both the stator at the rated speed are listed in Table 4.2. The simulated outer stator per phase voltage is found to be 1.549% higher than the experimental result. The rectified outer stator voltage is found to be 1.55% higher than the experimental DC voltage. Similarly, the inner stator phase voltage and the rectified voltage are found to be 1.156% and 1.15% higher than the experimental results respectively. Fig. 4.9 and Fig. 4.10 show the generated voltage and DC rectified voltage of the inner stator varying with rotor speed which is linearly related and the simulated results are in good agreement with the experimental results. Similarly, Fig. 4.11 and Fig. 4.12 show that the generated voltage and the DC rectified voltage of the outer stator winding varying with rotor speed and found to be linear in relationship and found the simulated results are in good agreement with the experimental.

Table 4.2 Analytical and experimental results of Stator Voltages.

Parameter	**Simulated (V)**	**Experimental (V)**
Outer stator phase voltage	227.47	224
Inner stator phase voltage	32.37	32
Outer stator DC rectified voltage	431.59	425
Inner stator DC rectified voltage	68.58	67.8

.

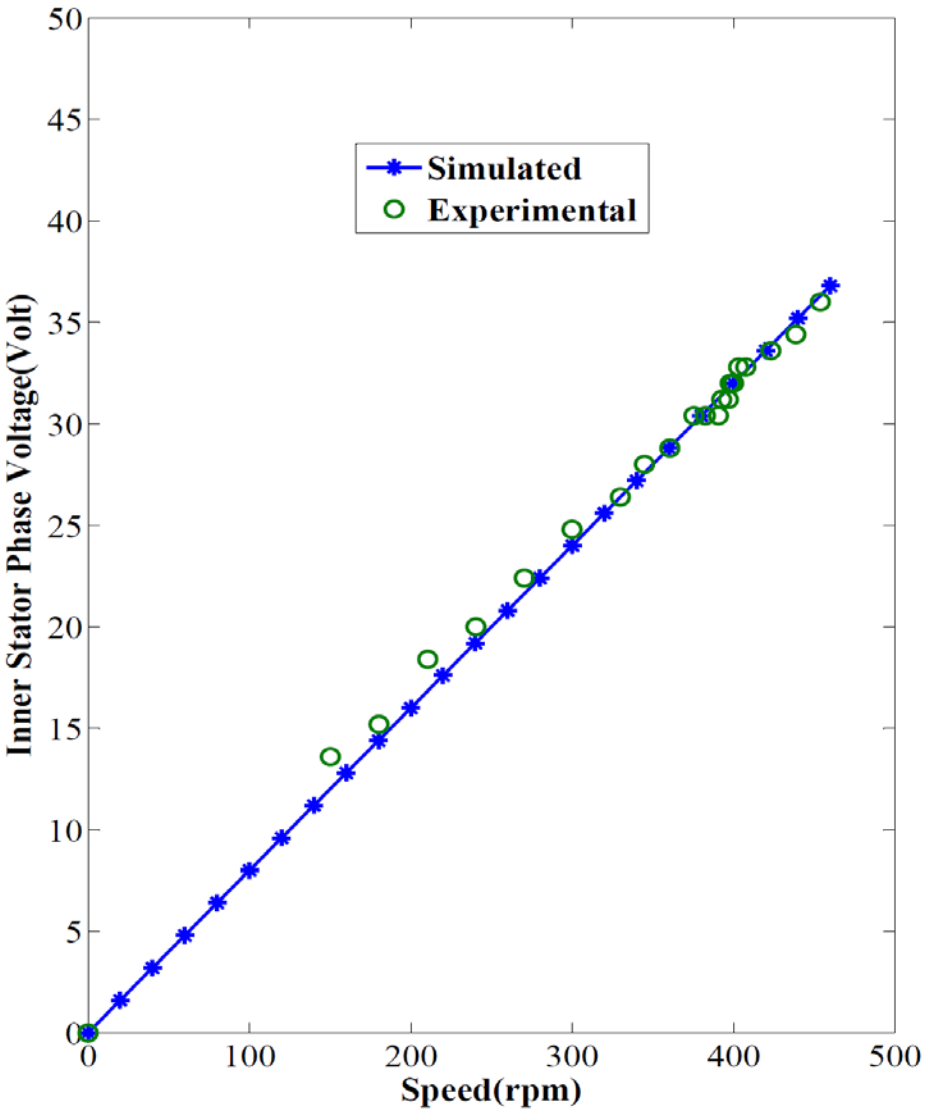

Fig. 4.9 Inner stator generated voltage of MCDSFP-PMSG

Fig. 4.13 shows the generated voltage of outer stator winding with varying rotor speed under healthy and faulty conditions. There are nine possible faults considered and the impact of these faults with respect to the healthy condition has been found. The faults are namely A-phase open, B-phase open, C-phase open, E-phase open, BC both phase open, BD both phase open, BCD three phase open, BCE three phase open, and BCDE four phase open from the rectified voltage circuits. Experimentally it is found that the performance under each faulty condition was degraded with respect to the healthy condition but the fault has been found to be severe with BCDE phase open.

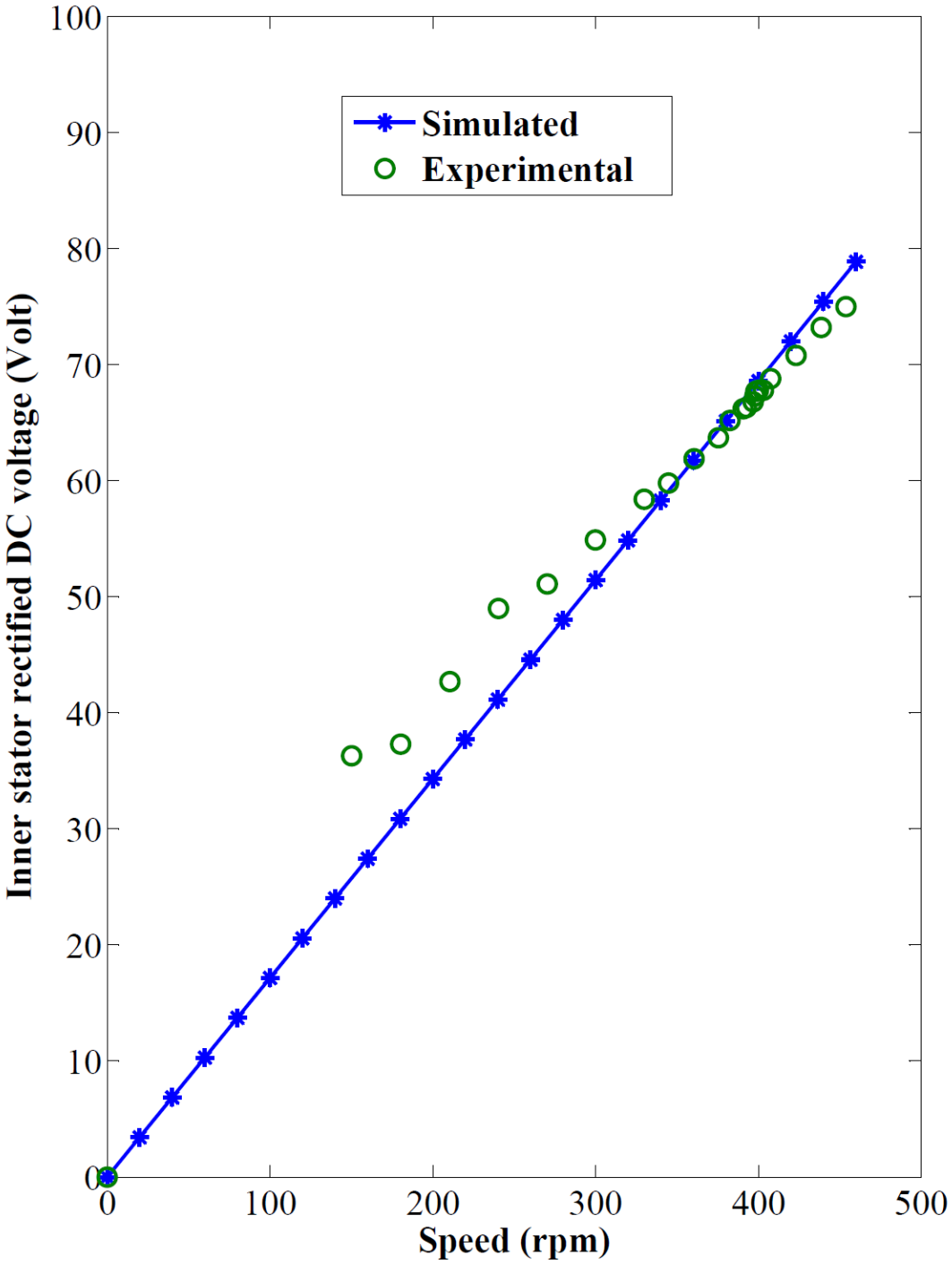

Fig. 4.10 Inner stator DC rectified voltage of MCDSFP-PMSG

.

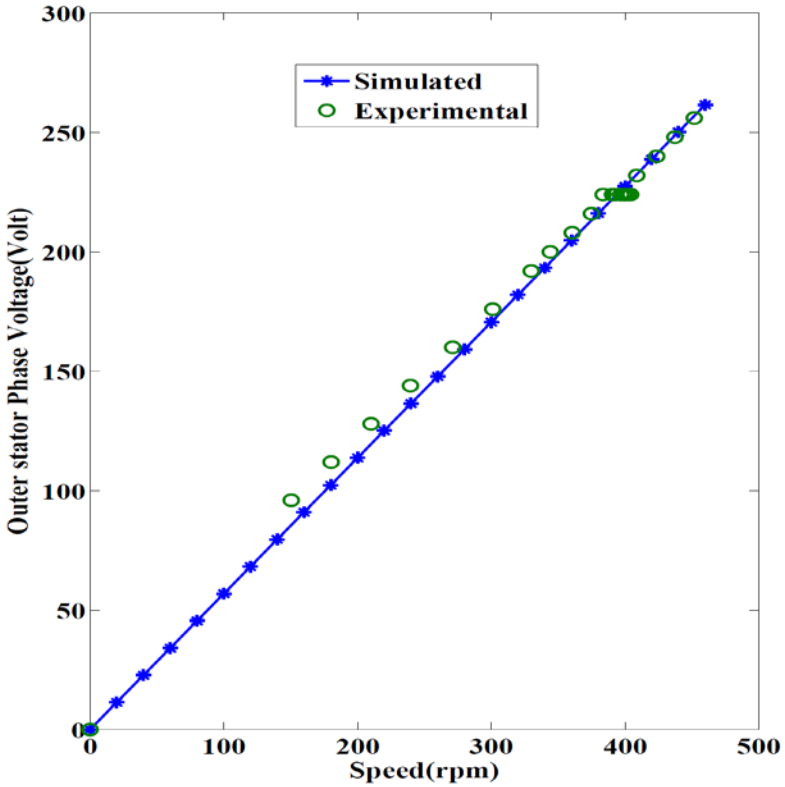

Fig. 4.11 Outer stator generated voltage of MCDSFP-PMSG

.

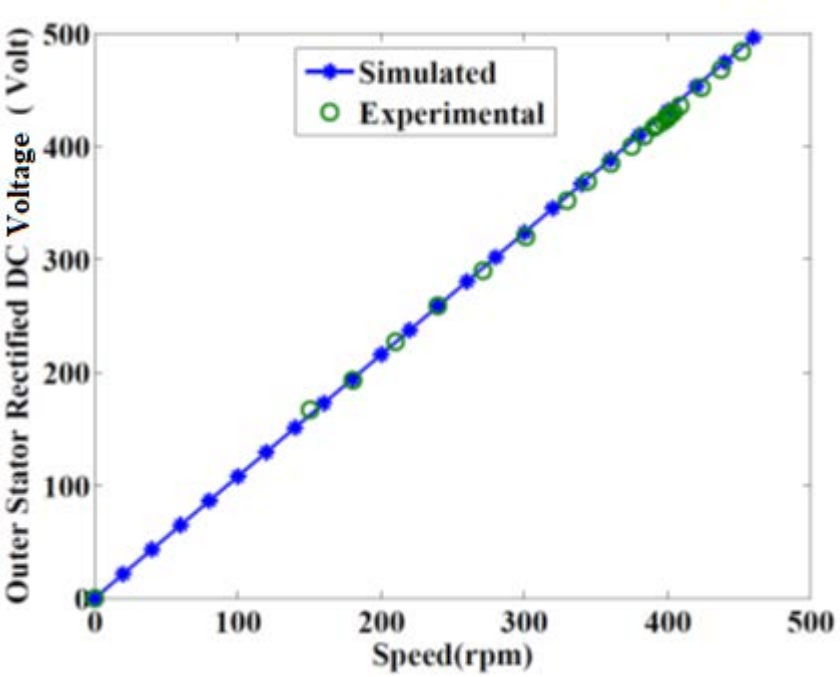

Fig. 4.12 Outer stator DC rectified voltage vs. speed under no-load condition of MCDSFP-PMSG

.

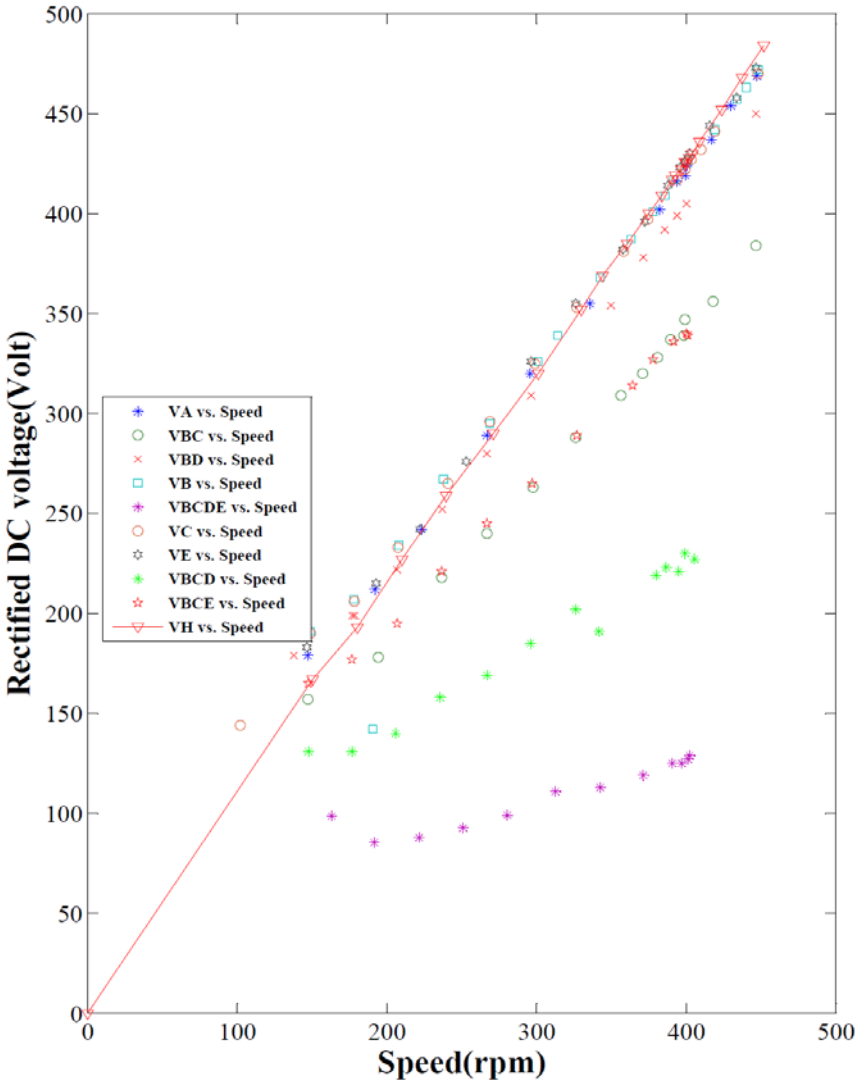

Fig. 4.13 Outer stator rectified voltage vs. speed under healthy and faulty condition

For extracting the load characteristic of MCDSFP-PMSG the generator is loaded with resistive load through five-phase diode rectifier circuit. The rectified DC voltages are found to be of drooping characteristic due to drop in the terminal voltage which depends on the generator parameters as shown in Fig. 4.14. The simulated results are in good agreement with the experimental results.

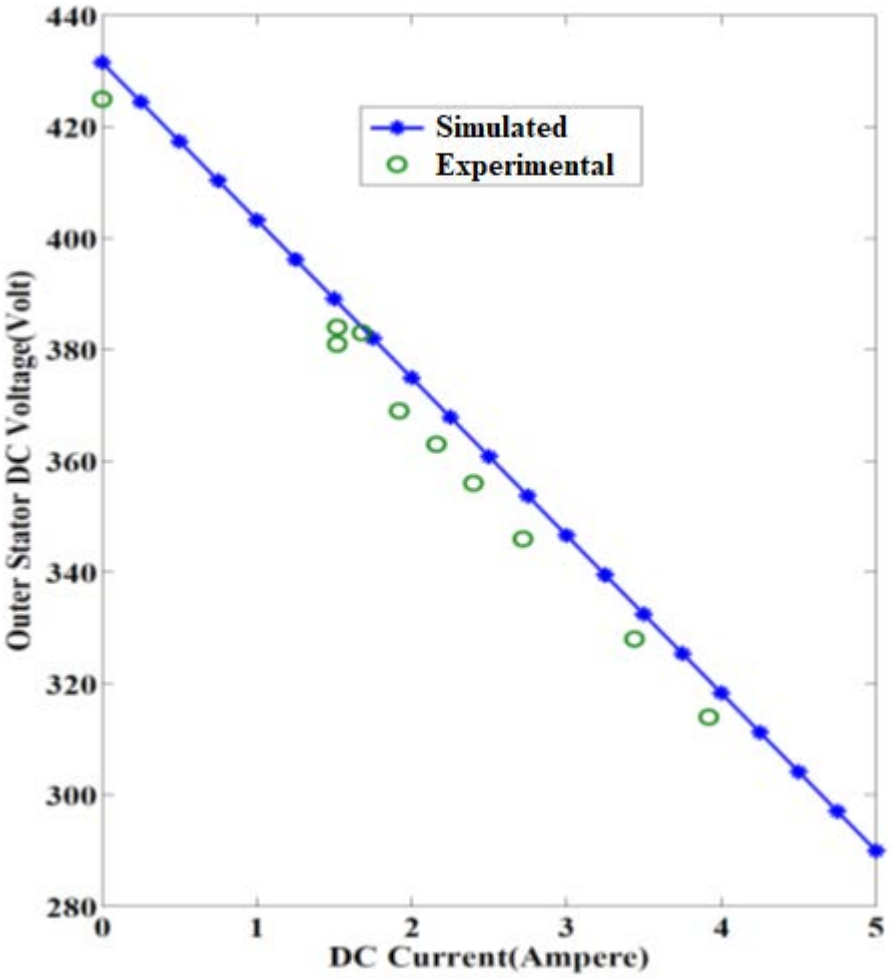

Fig. 4.14 Outer stator rectified DC voltage under loaded condition of MCDSFP-PMSG

Fig. 4.15 shows the DC rectified voltage of outer stator winding with the varying load under healthy and faulty conditions. There are nine possible open circuit faults considered and their impacts with respect to the healthy conditions are found. These faults are namely B-phase open, C-phase open, D-phase open, E-phase open, BC both phase open, BD both phase open, BE two-phase open, BCD three phase open, and BCE three phase open circuited. Experimentally it is found that the performance under each fault degraded with respect to the healthy condition but the fault is more predominant with BCD three phase open with the rectifier circuit.

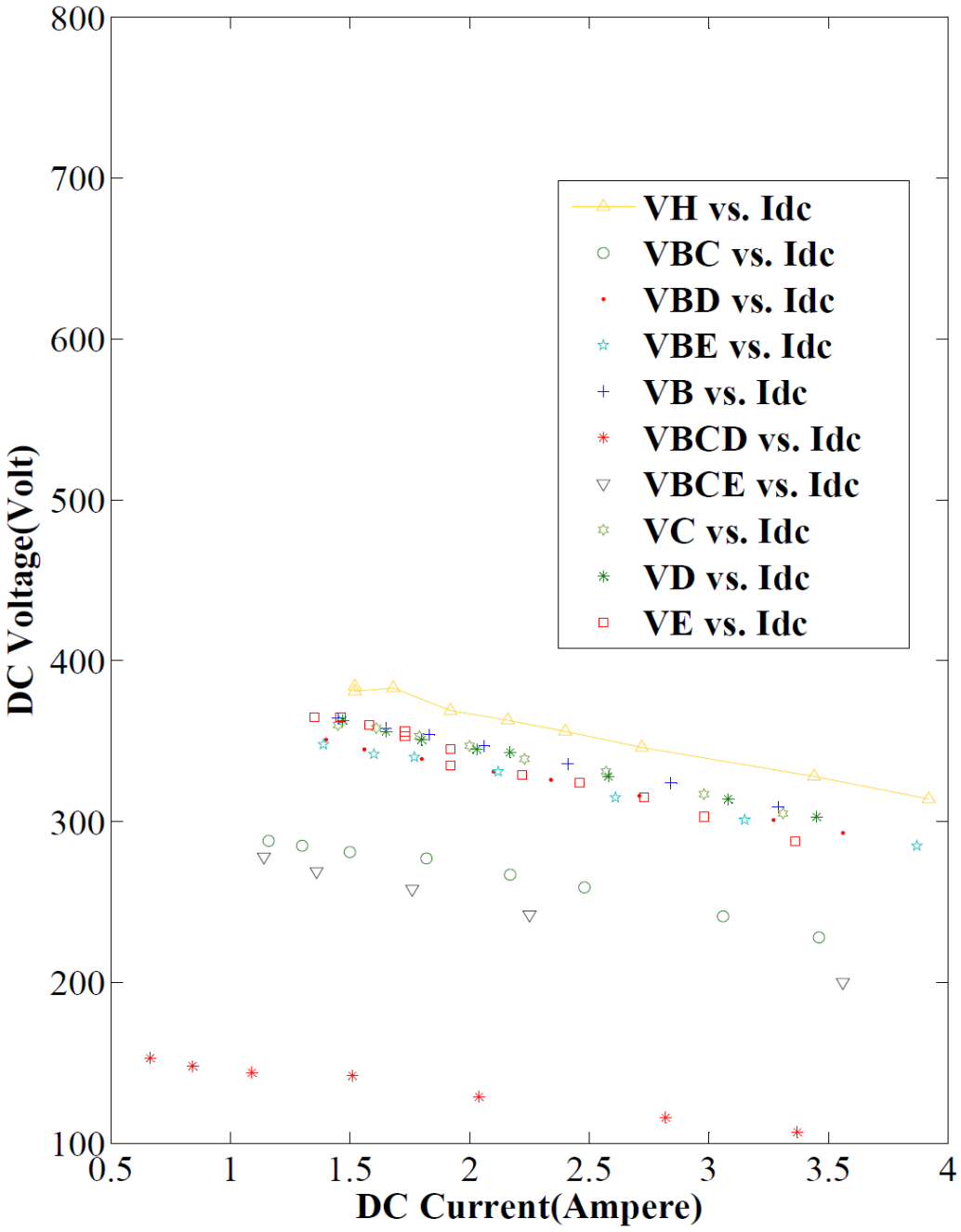

Fig. 4.15 Outer stator DC rectified voltage vs. DC current under healthy and faulty condition of MCDSFP-PMSG

4.4 Conclusion

The electromagnetic performance of SSFP-PMSG and MCDSFP-PMSG are evaluated analytically and validated with the experimental results. The result coming from analytical methods are found to be within the 5% of experimental results. The generated voltage and the rectified DC voltage are having linear relationship with varying speed. The load characteristic of the generated voltage is found drooping in nature. This is because of the generator parameter like phase resistances, inductances and armature reaction.

The fault like short circuit of winding (part or 100%) of one phase of multi-phase generators is rare and is beyond the scope of present work. Though in such case PM are to be safe guarded against possible demagnetization.

The Electromagnetic design cannot guarantee overall feasibility of generator alone, thus thermal modeling and optimization are deemed essential for predicting stability and desired performance of the generator.